Journal of The Electrochemical Society, 2026 **173** 147503

A Coupled Multi-Electrode Array Sensor for Monitoring Galvanic Corrosion Between Copper and Steel

Klara Kregar,[1] Miha Hren,[1] Aleš Nagode,[2] and Tadeja Kosec[1,z]

[1]*Slovenian National Building and Civil Engineering Institute, 1000 Ljubljana, Slovenia*
[2]*Faculty of Natural Sciences and Engineering, University of Ljubljana, 1000 Ljubljana, Slovenia*

The advanced coupled multi-electrode array (CMEA) technique provides spatiotemporal insights into electrochemical processes. This study used the CMEA technique to monitor the distribution of anodic and cathodic activity during galvanic interactions between copper and steel. An important parameter influencing the intensity of galvanic corrosion is the anode-to-cathode area ratio, which was also investigated. After exposure, corrosion products were analyzed using microscopic and spectroscopic techniques, and the extent of actual corrosion damage was evaluated using μ-CT. In the CMEA sensor with a Cu:CS ratio of 24:1, the corrosion rate of the CS electrode was estimated at 0.86 mm year^{-1} . For the area ratio of Cu:CS 22:3, a lower corrosion rate of 0.56 mm year^{-1} was observed for the CS electrodes. The influence of the reduction process on copper electrodes and the intensity of galvanic corrosion is demonstrated. The main corrosion products on the CS electrodes were goethite, lepidocrocite, and akaganeite, indicating a corrosion process involving oxygen. The copper electrodes acted as cathodes, but some individual Cu electrodes also exhibited anodic activity. This suggests simultaneous anodic and cathodic activity, and the anodic activity was confirmed by Raman spectroscopy, which detected the presence of Cu_2O. Cu_2S was also detected, indicating corrosion processes involving bisulfide ions.

[DOI: 10.1149/1945-7111/ae89ec]

Manuscript submitted May 18, 2026; revised manuscript received June 30, 2026. Published July 27, 2026.

Supplementary material for this article is available online

Galvanic corrosion occurs when two dissimilar metals are in contact in the presence of a corrosive electrolyte, where the driving force for corrosion is the potential difference between them.[1] In contact with a common electrolyte, a galvanic cell is formed, consisting of an anode, a cathode (more noble/positive metal), and a path for the electron current.[1,2] In the case of carbon steel (CS) coupled with copper (Cu), the more noble metal is Cu, based on the standard electrode potential,[3] so Cu acts as the cathode and CS as the anode.[1] Many parameters influence galvanic corrosion, including the properties of the materials, the solution conductivity, the temperature, the oxygen content, the stability of the oxide film, the distance between the coupled metals, and the area ratio of the anode to the cathode.[1,2,4] The greater the area ratio between the electrodes (small anode, large cathode), the more intense the galvanic corrosion is. The rate of galvanic corrosion depends on the rate of oxygen reduction as the main cathodic reaction ($O_2 + 2H_2O + 4e^- \leftrightarrow 4OH^-$).[1,2,5,6] Up to a Cu:CS ratio of 2500:1, the galvanic current (i_g) increases linearly, indicating on cathodic control with oxygen reduction.[5,6] Ziang et al.[7] investigated the evolution of i_g at Cu:CS area ratios from 3600:1–8000:1. The i_g remains constant, indicating on the shift of rate-determining step to anodic processes (CS oxidation). Li et al.[8] used a finite element analysis (FEA) model to predict the throwing power of Cu-to-CS galvanic couples at extreme area ratios (2.3×10^8:1–9×10^4:1). Bentonite generally reduced the throwing power, but when the exposed CS exceeded a critical dimension determined by bentonite thickness, throwing power increased due to enhanced oxygen reduction reaction kinetics on the reduced Cu cathode.

One proposed method for studying galvanic corrosion is the use of an advanced technique called the coupled multi-electrode array (CMEA) technique also known as wire beam electrode (WBE). The CMEA technique has been demonstrated to be a very useful and powerful tool for investigating non-uniform corrosion, such as localized corrosion (including the initiation and propagation of pitting), crevice corrosion, and galvanic corrosion, as well as for studying the statistical behavior of metal corrosion and evaluating inhibitors.[9–14]

The CMEA technique is unique for studying spatiotemporal evolution of corrosion processes on the surface being investigated. It is designed to simulate a larger surface area by galvanically coupling several smaller electrodes. The electrodes are galvanically coupled using a zero-resistance ammeter (ZRA), which ensures that no external current or potential is imposed. With no applied current or potential, the surface acts as a freely corroding surface, and real-time corrosion processes can be monitored in a simulated environment.[9,15,16] The CMEA method monitors the anodic and cathodic processes on individual electrodes. The anodic current of the most corroding electrode can be used to estimate the corrosion rate and represents a lower bound for the corrosion rate. This is because anodic and cathodic processes can occur simultaneously on the same electrode, so the corrosion rate may be underestimated.[16,17]

The multi-electrode array technique is widely used to investigate localized corrosion, as conventional electrochemical techniques are not suitable due to the complexity of anodic and cathodic sites interactions.[13,14] Using electrode arrays, it was shown that the ohmic potential drop near an active pit produces the strongest suppression of electrochemical activity on immediately adjacent passive electrodes, with the effect diminishing systematically toward the array's edge, where susceptibility is highest.[18,19] Parvizi et al.[20] employed the multi-electrode array technique with 1 mm and 100 μm wires to investigate localized corrosion processes over heterogeneous metal surfaces on AA2024-T3. It was demonstrated that electrode size determines which stage of corrosion is captured. Wires with a 100 μm diameter revealed early-stage corrosion initiation activities among intermetallic particles, which larger wire sizes cannot detect.[20] Using the concept of a three-dimensional electrode array, Laleh et al.[21] demonstrated the technique's capability for investigating internal pipeline corrosion under various environmental conditions and investigation of corrosion influencing factor such as differential aeration, pH and inhibitors.

Previous work has shown that the CMEA technique can be used to study the electrochemical inhomogeneity of zinc in a zinc/steel galvanic couple in seawater. The spatiotemporal distribution of anodic and cathodic currents was demonstrated, as anodic activity moved between the zinc wires to mild steel and then to the furthest zinc wires in the sample.[22] The galvanic throwing power of

[z] E-mail: tadeja.kosec@zag.si

bare and polymer-coated Mg over bare AA2024-T351 substrates under various immersion conditions, different thin layers, and droplet electrolyte geometries was studied with CMEA. Several parameters influence the throwing power, including the thickness, chemistry, and geometric area of coverage of the electrolyte layer and it was limited by the reduction in the length of ionic conductive pathways during wet and dry cycles.[23] Another study investigated interactions between aluminum alloy and stainless steel under atmospheric exposure, represented by thin electrolyte films and wet/dry cycles. It was shown that the current increased at the onset of wetting and drying due to the high concentration of Cl^- in the droplet and the thin electrolyte layer. A higher galvanic current density indicates a faster corrosion rate of the aluminum alloy.[24]

Galvanic corrosion between Cu and CS has primarily been studied in the context of deep geological repositories (DGR), which is an internationally accepted concept for the permanent storage of spent nuclear fuel. In the Canadian concept, spent nuclear fuel will be stored in CS containers that provide mechanical strength. These containers will be coated with a 3 mm layer of Cu to provide corrosion protection in the DGR environment.[25–27] If a defect in the Cu coating goes undetected, which is technically confirmed to be highly unlikely, the underlying steel could be exposed to the DGR environment, resulting in CS being galvanically coupled to Cu. This can lead to galvanic corrosion.[5,28] Galvanic corrosion has been investigated using a simulated through-coating defect and analyzed using microtomography. It was observed that the corrosion of CS propagated along the Cu–CS interface.[29] Another study investigated the influence of the Cu:CS area ratio in different chloride concentration solutions by monitoring the galvanic current and coupled potential. It was found that galvanic corrosion is influenced by the cathodic reaction on Cu (the reduction of oxygen) and that the corrosion rate increased as the surface area ratio between Cu and CS increased.[5]

An additional engineering barrier will be used in the DGR which will provide further protection for the container. This will involve the use of compacted bentonite clay, which limits the transport of groundwater and corrosive species to the surface of the container. The presence of bentonite also limits the reduction of O_2 on Cu, which influences the intensity of the galvanic current density on CS.[6,30,31] Study with a micro-reference electrode array examined the throwing power of a Cu-to-CS galvanic couple in a NaCl solution with and without bentonite. In the presence of bentonite, the throwing power measured initially peaked, but it then declined to values even lower than those observed in the solutions without bentonite. Compacted bentonite will be used in the DGR, and it is expected that the Cu-to-CS throwing power will be even lower.[8]

To monitor the galvanic corrosion between Cu and CS, Kosec et al.[32] used the CMEA technique to observe galvanic interactions between Cu and CS in both a simulated solution and bentonite slurry. The average current density for the CS electrode in the simulated solution was 1490 $\mu A\ cm^{-2}$, resulting in a corrosion rate of 17 mm $year^{-1}$. In the bentonite slurry, the average current density of CS was 114 $\mu A\ cm^{-2}$, resulting in a corrosion rate of 1.3 mm $year^{-1}$.[32]

Since the container will be stored in the DGR for a long period (10^6 years),[27] there is a significant need for long-term monitoring of the corrosion processes. The aim of this investigation was to monitor the long-term galvanic interactions between Cu and CS under the influence of a bentonite mixture in an oxic environment. Initially, oxic conditions will exist in the DGR (estimated to be around 100 years). Oxygen will be trapped when the containers are deposited in the DGR and will be used for the oxidation of minerals in the bentonite and for oxidation of the copper coating.[25] On the early corrosion stages, the presence of bisulfide (SH^-) ions also influences the corrosion processes.[33] The SH^- concentrations in the groundwater are anticipated to range between 10^{-6} M and 10^{-4} M.[25]

This study provides new insights into the mechanism of galvanic corrosion by combining long-term exposure to relevant repository conditions with spatiotemporally resolved electrochemical measurements. Unlike previous, short-term studies, this approach can characterize the evolution of the intensity of anodic and cathodic processes during the long-term monitoring of galvanic corrosion between copper and steel. As the surface area ratio between Cu and CS influences corrosion, the CMEA technique was also used to assess this effect.

Following the period of exposure, various spectroscopic techniques were used to analyze the types of corrosion products formed on the surface. The extent of the damage was also evaluated by μ-CT, which enabled validation of the corrosion depth assessment obtained from the average current values during long-term exposure using the CMEA sensing technique.

Experimental

Materials and preparation.—Two different sets of sensors were built for the coupled multi-electrode array (CMEA) technique to continuously monitor the anodic and cathodic currents (Fig. 1b). The CMEA sensor consisted of 25 electrodes arranged in a 5×5 grid (Fig. 1a). The electrodes were embedded in epoxy resin and placed in a 3D-printed housing. Each electrode had a diameter of 0.5 mm with an exposed surface area of 0.196 mm^2. The edge-to-edge spacing between the electrodes was 0.5 mm. The CMEA-CS-1 sensor was fabricated from 24 copper (Cu) electrodes with a purity of 99.99 wt.% (purchased from Goodfellow, Huntingdon, England, UK) and 1 carbon steel (CS) electrode, whose chemical properties were verified by optical emission spectroscopy (as shown in Table S1 in the Supplementary Material). The copper wire was insulated with polyimide to prevent crevice corrosion between the wires and the epoxy resin. The CMEA-CS-1 sensor represented possible damage to the container, with a Cu/CS ratio of 24/1. The second sensor, CMEA-CS-3, was geometrically identical but constructed from 22 Cu electrodes and 3 CS electrodes, equating to a Cu/CS ratio of 22/3, thus representing a larger area of carbon steel in relation to the area of copper.

Before exposure, both sensors were ground with 600–4000 grit SiC paper, polished with 1 μm diamond paste, ultrasonically cleaned in deionized water for 3 min, and dried in a stream of air.

The bentonite mixture was poured into a 3D-printed pool affixed to the sides of the CMEA sensor electrodes. The mixture was prepared using a 1:1 bentonite to solution ratio, with 20 g of Wyoming MX-80 bentonite mixed with 20 ml of a 0.2 M Cl^- solution containing a low concentration of sulfide (5×10^{-6} M SH^-). NaCl ($\geqslant$ 99.5%, Fisher Chemical) was used to prepare the 0.2 M chloride solution, and $Na_2S{\cdot}9\ H_2O$ (98 + %, Carlo Erba) was used to prepare the sulfide solution. All chemicals were of p.a. grade. The solution was freshly prepared before each experiment under oxic conditions. The pH of the solution was 7.1 and the dominant sulfide species is the bisulfide ion.[34,35]

Monitoring technique.—The CMEA technique was used for the continuous long-term monitoring of currents in the 25-electrode sensors. CMEA provides spatiotemporal insight into corrosion processes and allows natural corrosion processes taking place at the surface to be monitored. The CMEA-CS-1 sensor, representing galvanic corrosion with a ratio of 1/24, was monitored for 186 d, while the CMEA-CS-3 sensor, with a CS/Cu ratio of 3/22, was monitored for 176 d. This study evaluates galvanic corrosion in the bentonite mixture during the oxic period, when oxygen is present. A temperature of 22 ± 2 °C and a humidity of 30% were maintained throughout the exposure period. The sample was covered with parafilm and a 3D-printed cover to minimize drying of the bentonite and prevent the ingress of oxygen.

The sensors were connected to a custom-made zero-resistance ammeter (ZRA) built in the laboratory. All the electrodes were galvanically coupled without the application of any external potential or current. The anodic (positive) currents represent anodic activity (the oxidation process), and the cathodic (negative) currents represent cathodic activity (the reduction process). The detectable current

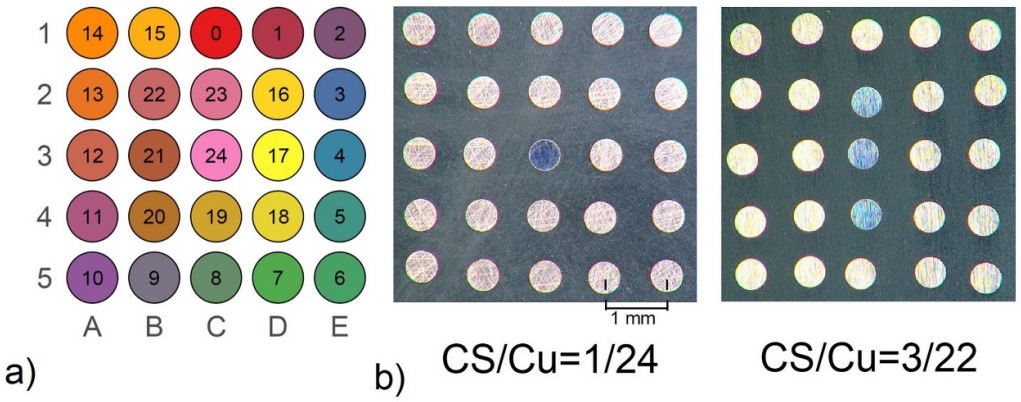

Figure 1. (a) Color matrix of the 5×5 grid and (b) the two different CMEA sensors with different CS ratios.

range of the ZRA device was from −5 μA to + 5 μA, with a precision of 150 pA per electrode. The frequency was set to 1 Hz throughout the entire exposure period. The anodic currents measured were converted to normalized anodic current densities (μA cm^{-2}) using an electrode surface area of 0.196 mm^2. For a clearer visualization of the evolution of the current density over the entire exposure time, the measurements were time-averaged, with each data point representing the average over a 100 s interval.

The corrosion rate (v_{corr} [μm year^{-1}]) was calculated from the normalized anodic current density (j_{corr} [μA cm^{-2}]) using Equation 1, where 3.27 is a constant obtained from Faraday's law (μm g μA^{-1} cm^{-1} year^{-1}), M is the molar mass (g mol^{-1}), ρ is the density (g cm^{-3}), and z is the number of electrons required to oxidize the atom,

$$v_{corr} = j_{corr}\frac{3.27M}{\rho z}. \quad [1]$$

The damage to individual electrodes can be calculated from the normalized anodic current densities obtained using Eq. 2, where d represents the corrosion damage, t is time (s), and F is the Faraday constant (96485 C mol^{-1}),

$$d = \frac{j_{corr}Mt}{\rho zF}. \quad [2]$$

Surface characterization.—At the end of the exposure, the bentonite mixture was removed and the surfaces of the CMEA sensors were rinsed with deionized water and dried in air. First, the CMEA sensors were analyzed using Raman spectroscopy. This non-destructive technique provides chemical information about the composition of corrosion products without the need for sample preparation. The corrosion products were analyzed using a Horiba Jobin Yvon LabRAM HR800 Raman spectrometer coupled with an Olympus BXFM optical microscope. To obtain Raman spectra, a 633 nm laser excitation line, a 100 × objective lens, and a 600 grooves mm^{-1} grating were used. The elemental composition and morphology of the corrosion products were examined using a ThermoFisher Scientific Quatro S (Hillsboro, OR, USA) field emission scanning electron microscope (FEG SEM) connected to an EDS SDD Ultim® Max detector (Oxford Instruments). FEG-SEM/EDX analyses were performed at an accelerating voltage of 15 kV. Prior to analysis the sensors were coated with carbon to enable conductivity of the electrode surfaces embedded in the non-conductive epoxy.

To analyze damage to the electrodes, a non-destructive 3D imaging technique, X-ray micro-computed tomography (μ-CT), was used. An EasyTOM XL Ultra system was used to perform the analysis and obtain a 3D image of the CMEA electrodes. The X-ray source was set to a voltage of 160 kV and a power of 6.7 W. A 0.35 mm copper filter was used. The source-to-object distance (SOD) was set to 35.12 mm, and the source-to-detector distance (SDD) was 897.72 mm, resulting in a voxel size of 5 μm. The software Dragonfly 2024.1 was used to process the data obtained from μ-CT. First, the CMEA electrodes were segmented using interactive thresholding and a 3D image of each electrode was obtained, then the binary image of the damaged electrode was subtracted from that of the reference electrode (cylinder). The cylinder represented the volume of the original, undamaged electrode. By dividing the corroded volume by the surface area of the electrode, the average corrosion depth was calculated.

After characterizing the corrosion products on the electrode surfaces, the corrosion products and residual bentonite that could not be removed with deionized water were eliminated to analyze the underlying surface. The corrosion products on the copper, bentonite, and carbon layer were removed using a solution of HCl:H_2O = 1:1 with 3.5 g l^{-1} $C_6H_{12}N_4$, then rinsed with deionized water and dried with a stream of air. Damage to the copper electrodes was analyzed using a JEOL JSM-IT500 electron microscope equipped with an Aztec Live Advanced ULTIM 65 EDXS detector (Oxford Instruments, Abingdon, UK). The electrodes were examined at an accelerating voltage of 15 kV. The surfaces of the steel electrodes were not analyzed because the solution used to remove the corrosion products and bentonite residue caused etching.

Results and Discussion

The results from analysis of the coupled multi-electrode array sensors are presented below. The two different CMEA sensors with varying Cu:CS ratios were exposed to a bentonite mixture in an oxic environment and the spatio-temporal distribution of the currents on 25 electrodes (Cu, CS) was monitored. The system acts as a freely corroding surface, and a natural corrosion system can be simulated. Two sensors, representing copper-steel galvanic couples, were exposed to the bentonite mixture in oxic conditions for either 186 d (CMEA-CS-1 sensor) or 176 d (CMEA-CS-3 sensor).

Continuous monitoring of the CMEA-CS-1 sensor with a Cu to CS ratio of 24/1 under a bentonite mixture in an oxic environment.—The results from the continuous monitoring of the CMEA-CS-1 sensor with a Cu/CS ratio of 24/1 are shown in Fig. 2. The currents of the CMEA-CS-1 sensor were monitored for 186 d under a bentonite mixture in an oxic environment.

After pouring the bentonite mixture over the CMEA-CS-1 sensor, the anodic peak of the C3 steel electrode first increased to more than 450 μA cm^{-2}, as shown in Fig. 2a. The anodic current density decreased relatively quickly, and after 16 d the activity of the CS electrode C3 fell below 10 μA cm^{-2}, maintaining stable anodic current activity throughout for the next 28 d of exposure. The decrease

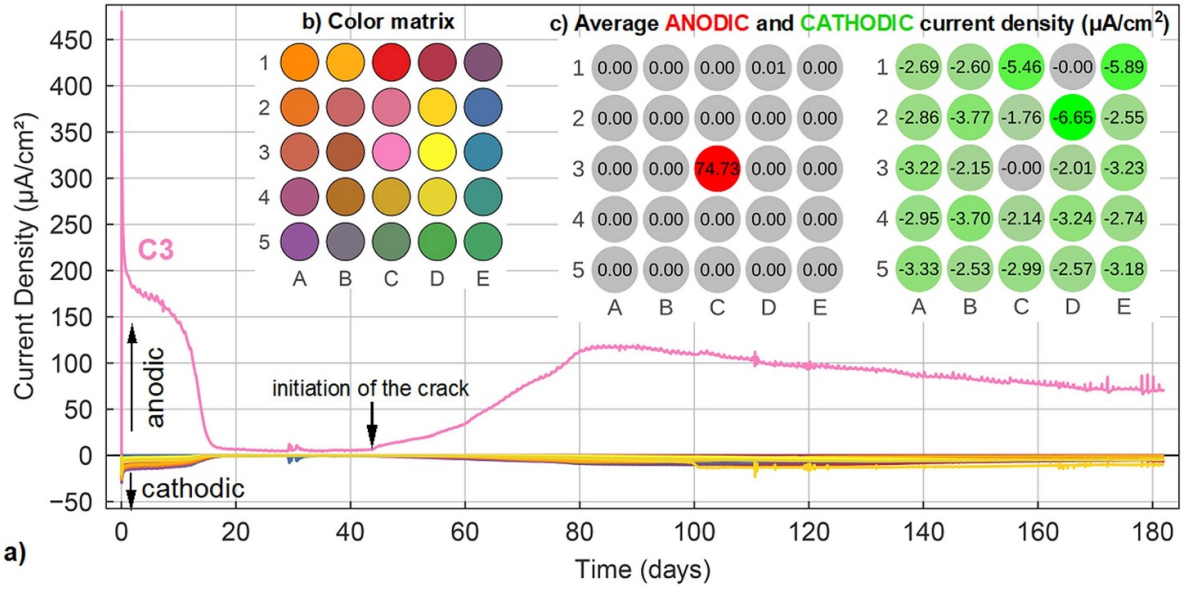

Figure 2. (a) Evolution of the current densities in CMEA-CS-1 sensor with a Cu/CS ratio of 24:1 over 186 d of exposure to the bentonite mixture in an oxic environment; (b) color matrix of a 5 × 5 grid, and (c) average anodic and cathodic current densities of individual electrodes.

in anodic current density could be due to the mixture of corrosion products and the presence of bentonite, which limit the transport of corrosive species to the steel electrode and the transport of the cathodic reactant, O_2, to the copper electrodes.[6]

During the next 43 d of exposure (day 45 to day 87), the bentonite mixture may have started to dry out, as indicated by visible cracks around the edges of the pool that were observed at the end of the exposure period. These cracks likely facilitated oxygen diffusion through bentonite to the electrodes, which is reflected in the steady increase in anodic current density of the C3 CS electrode, rising to over 115 μA cm^{-2}. This increased oxygen diffusion promoted the cathodic oxygen reduction reaction, resulting in greater anodic dissolution of the carbon steel. After this peak, the anodic current density began to slowly decrease over the next 96 d of exposure (from day 87 to day 183). This could be attributed to the accumulation of corrosion products, which can limit the corrosion rate of CS. At the end of the exposure, the anodic current density of the C3 steel electrode was 70 μA cm^{-2}.

The corrosion rate was estimated using the anodic current density from the most corroded electrode (C3). The CMEA technique can underestimate the corrosion rate if anodic and cathodic sites form on the same electrode and internal electron flow occurs. If both reactions occur on the same electrode, the actual corrosion rates are underestimated, whilst the corrosion rate obtained from anodic currents represents the lower bound of the corrosion rate and does not reflect the actual corrosion conditions.[15–17] In highly corrosive environments such observations are less expressed.

The average anodic and cathodic current densities of the electrodes over 186 d of exposure are shown in Fig. 2c. The average anodic current density for the C3 steel electrode was 74.7 μA cm^{-2}. The corrosion rate was calculated using Eq. 1. The estimated corrosion rate of the C3 steel electrode over 186 d was 0.86 mm year^{-1}.

Galvanic corrosion in the early oxide phase has previously been investigated using the CMEA technique on a sensor with a Cu/CS ratio of 24:1 under bentonite slurry. The sensor was exposed for 13 d, with the corrosion rate of the CS electrode being 1.3 mm year^{-1} .[32] A denser bentonite mixture was used in our study, which contributed to a lower galvanic intensity by more efficiently inhibiting O_2 transport. In both studies, the main driving force of galvanic corrosion under oxide conditions was oxygen reduction.

Using μ-CT tomography, the CMEA-CS-1 sensor was analyzed to measure the volume of corrosion damage. The data obtained through μ-CT can be used to assess the overall corrosion damage and to compare this with the data obtained using the CMEA technique. The total damage volume of the C3 CS electrode obtained from μ-CT was 92.5·10^6 μm^3, which corresponds to a total electrode damage of 471 μm. The volume damage measured by the CMEA technique was 80.4·10^6 μm^3, corresponding to approximately 425 μm of corrosion damage. Slightly higher corrosion damage was, therefore, measured by μ-CT. This may indicate that anodic and cathodic processes simultaneously occurred on the same electrode with the current density measured being the net anodic current density. It was previously reported that if large differences exist between the results, the individual electrodes are strongly influenced by simultaneous anodic and cathodic processes on the same electrode surface; therefore, the corrosion rate determined by the CMEA method is a lower bound of the corrosion rate.[17] This suggests that corrosion damage, and consequently the corrosion rate, was slightly underestimated for the C3 CS electrode. The damage measured by μ-CT was approximately 10% higher than the value obtained by the CMEA technique.

Scanning electron microscopy (SEM) and Raman spectroscopy were performed to characterize the corrosion products on the surfaces of the electrodes after exposing the CMEA-CS-1 sensor to a bentonite mixture in an oxic environment. The surface characterization of the C3 CS electrode in the CMEA-CS-1 sensor is shown in Fig. 3.

As shown in Fig. 3a, visible cracks are observed on the surface of the C3 CS electrode, and, at a higher magnification, the morphology of the corrosion products can be seen. The corrosion products appear as small, aggregated corrosion deposits with a very dense texture. EDX analysis of the corrosion products was performed, and the presence of iron oxides as well as bentonite residue was detected. Similar observations were made at locations 1 and 2. The Fe content was ≈ 55 wt.%, O content ≈ 30 wt.%, Ca content ≈ 3.7 wt.%, Na content ≈ 1.5, Si ≈ 2.4 wt.%, and S ≈ 2.6 wt.%. The other elements identified by EDS analysis at sites 1 and 2 were Mg, Al, and P, all of which were under 1 wt. %. Fe oxyhydroxides were the major corrosion product, with the remains of bentonite residue.

Following the period of exposure to a bentonite mixture in an oxic environment, Raman spectroscopy was performed on the C3 CS

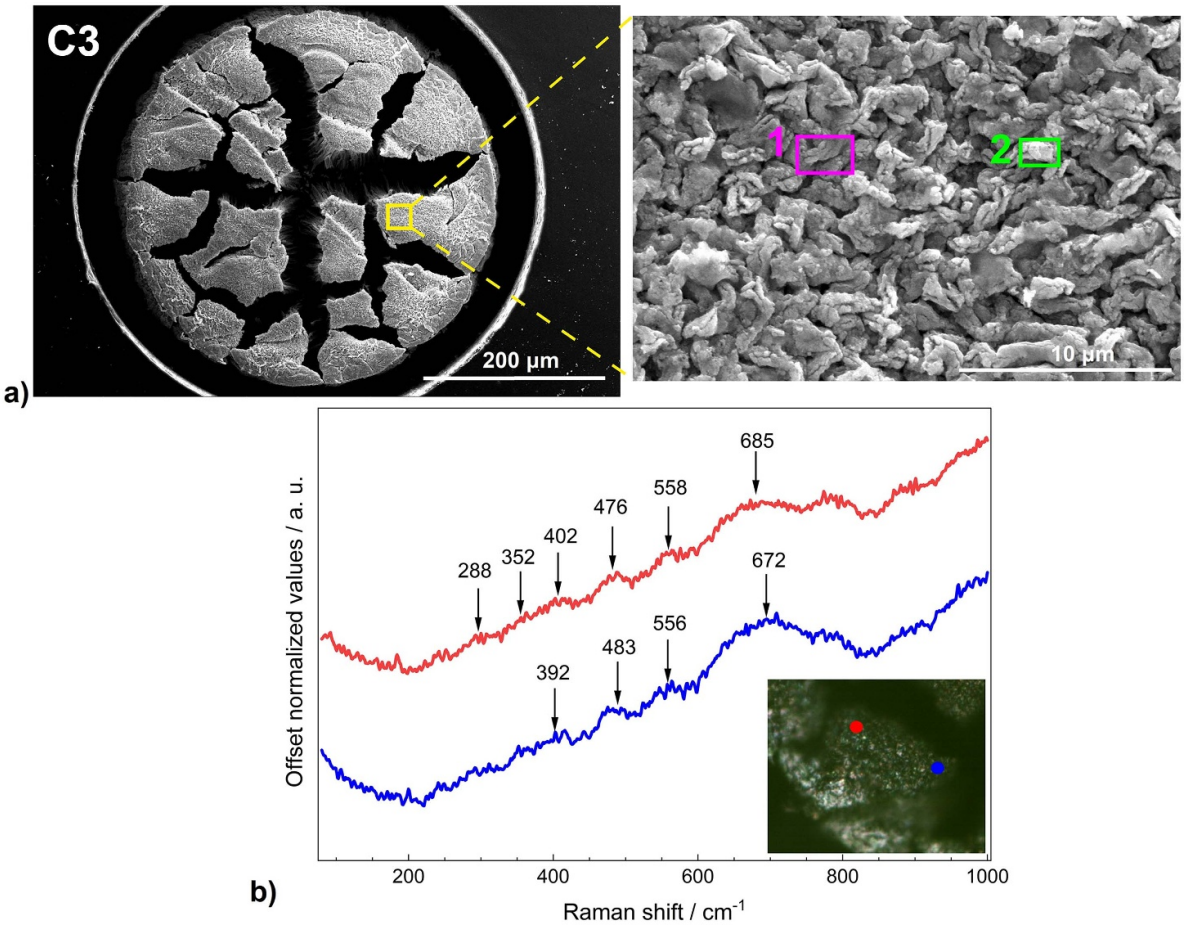

Figure 3. (a) SEM/SE images of the C3 CS electrode at 230 × and 5000× magnification, and (b) Raman spectra of the C3 CS electrode after exposure to the bentonite mixture in an oxic environment for 186 d.

electrode to specify the type of corrosion products. As shown in Fig. 3b, analysis of the surface confirms the presence of a corrosion film composed of iron oxyhydroxide. The Raman spectra indicated the presence of goethite[36] (α-FeOOH), with bands at 288 cm^{-1}, 352 cm^{-1}, 402 cm^{-1}, 476 cm^{-1}, 558 cm^{-1}, and 685 cm^{-1}. The presence of goethite indicates the formation of a protective iron oxyhydroxide which can inhibit the diffusion of the cathodic reactant to the CS electrode,[4,37] consistent with the observed gradual decrease in anodic current density after day 87.

When examining the copper electrodes, those closest to the CS electrode do not experience the highest cathodic current densities because oxygen reduction on copper is diffusion controlled. Dissolved oxygen is quickly consumed near the CS electrode, causing the diffusion-limited current density to decrease as O_2 is depleted. As shown in Fig. 2c, the copper electrodes B3, C2, C4, and D3, which are nearest to the CS electrode, have average cathodic current densities between –1.76 μA cm^{-2} and –2.15 μA cm^{-2}, while the edge copper electrode E1 has an average cathodic current density of –5.89 μA cm^{-2}. This behavior is consistent with the distribution of ohmic potential drop, which, as demonstrated by Newman et al.[38] is concentrated close to an active electrode. Consequently, passive electrodes near the anode are subject to the largest local potential perturbation, while those farther away are progressively less affected.[38] Similar observations were reported, where the electrodes nearest to the active electrode exhibited suppressed activity due to a combination of local oxygen depletion and ohmic drop in the electrolyte.[12,32]

The two most distinct of the 24 copper electrodes were analyzed: the D1 copper electrode, which showed the net anodic activity throughout the exposure, and the D2 copper electrode, which had the lowest net cathodic current density. The electrodes D1 and D2 are neighboring electrodes located north of the C3 steel electrode. The SEM images and current density evolution for these two electrodes are shown in Fig. 4.

The D1 copper electrode is the only copper electrode that showed very low net anodic activity, at $\pm$0.05 μA cm^{-2}. The evolution of the current density for the D1 copper electrode is shown in Fig. 4c. Net anodic activity is almost negligible, and the change in current density over time clearly indicates that both anodic and cathodic processes occurred on the same electrode surface, so the current density represents the net current density. Consequently, the average net anodic current density over the period of exposure was 0.01 μA cm^{-2}, resulting in 0.12 μm of damage to the electrode. The estimated corrosion rate of the D1 copper electrode was 0.23 μm $year^{-1}$. The net anodic behavior of the D1 copper electrode was unexpected, as all copper electrodes should act like cathodes in galvanic corrosion, where oxygen reduction occurs. It can be assumed that because of oxygen depletion and potential ohmic drop, local environment established across copper electrode D1. The net anodic activity observed on the D1 copper electrode indicates the oxidation of the copper surface. Surface characterization can confirm this assumption about the corrosion processes on the copper surface if the presence of cuprite is confirmed.

Other copper electrodes exhibited net cathodic activity. The most cathodic were the copper electrodes D2, E1, and C1, which are positioned around the D1 copper electrode. The electrode with the lowest cathodic current density was the D2 copper electrode (evolution of

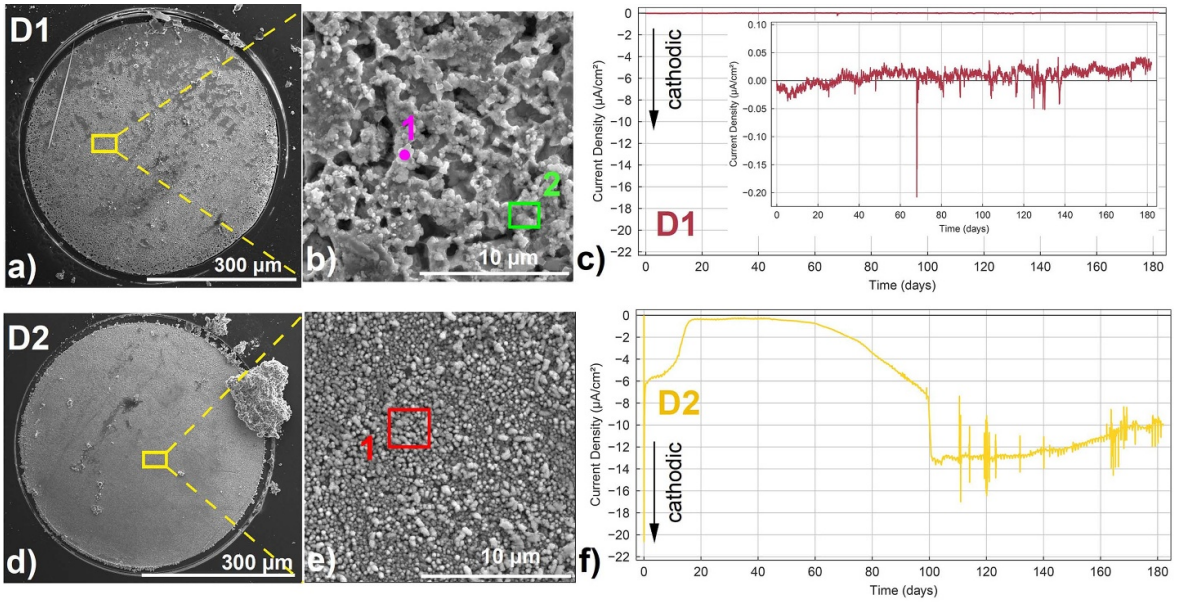

Figure 4. SEM/SE images of the D1 copper electrode (a), (b) with the EDX spots, evolution of current density for the D1 copper electrode (c), SEM images of the D2 copper electrode (d), (e) with the EDX spot, and evolution of current density for the D2 copper electrode (f).

current density shown in Fig. 4f), with an average cathodic current density of –6.65 μA cm^{-2}.

Figure 4 presents the SEM characterization with EDX spot analysis of the surface of the anodic D1 copper electrode (Figs. 4a and 4b) and the most cathodic copper electrode, D2 (Figs. 4d and 4e), after exposure to a bentonite mixture in an oxic environment.

As shown in Fig. 4b, the surface of the D1 copper electrode is covered with larger corrosion products, indicating the net anodic activity of the electrode and ongoing anodic processes. The surface appears rougher and more porous. Fine agglomerates have formed on top of the large corrosion products. EDS analysis was performed at two spots. At spot 1, a high Cu content (average 96 wt.%) was detected, along with a small S concentration (0.4–1 wt.%) and a lower concentration of O (2.3–3.6 wt.%). At spot 2, higher S and O concentrations were observed (3.4–4 wt.% S and 5.8–6.4 wt.% O), while the Cu content was lower, at approximately 90 wt.%.

In contrast to the D1 copper electrode, the D2 copper electrode was covered with much smaller corrosion products, such as crystals, as shown in the SEM image in Fig. 4e. EDX analysis revealed that the surface is covered with corrosion products consisting of a high copper content (average 96 wt.%), O (average 3 wt.%), S (average 0.5 wt.%), and Si (average 0.14 wt.%).

Raman spectroscopy was performed to analyze the corrosion products on the D1 and D2 copper electrodes D1 and D2 and is shown in Fig. 5.

The Raman spectra of both the D1 and D2 copper electrodes identified cuprite (Cu_2O), with bands at 145 cm^{-1}, 217 cm^{-1}, 530 cm^{-1}, and 624 cm^{-1}, indicating corrosion processes involving oxygen. A broad band at 287 cm^{-1} was observed on both samples, indicating the presence of chalcocite (Cu_2S). This confirms that corrosion involving SH^- ions occurred at the copper surface, despite possible oxidation of the bisulfide solution and possible reaction with bentonite. The broad Cu_2S peak indicates poor crystallinity of the corrosion products, which is attributed to the thick bentonite layer.[6,39] This band was more pronounced on the D1 electrode, which exhibited higher net anodic activity, indicating a greater amount of sulfur-containing corrosion products on this electrode. This was also observed in the EDX analysis, where the corrosion products on the surface contained more sulfur (average 6 wt.%). The presence of Cu_2S on the D2 copper electrode may indicate the overall activity of

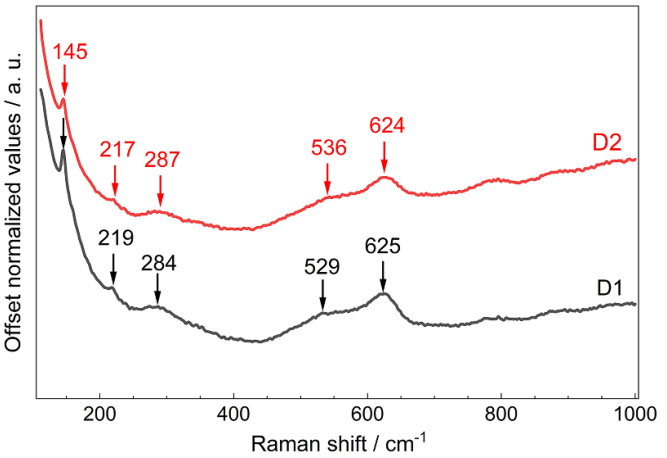

Figure 5. Raman spectra of the D1 (net anodic behavior) and D2 (net cathodic behavior) copper electrodes after exposure to the bentonite mixture in an oxic environment for 186 d.

the electrode, where not only the oxygen reduction process occurred but also anodic processes such as oxidation of the copper surface and reactions with bisulfide ions.

If anodic processes occurred only on the C3 carbon steel electrode, the copper electrodes would not be damaged. However, SEM revealed damaged surfaces on the copper electrodes, and Raman spectroscopy identified the corrosion products as Cu_2O and Cu_2S. Therefore, we can conclude that anodic processes also occurred on the surfaces of these electrodes. More intense processes were observed on the D1 copper electrode, where the current density development indicated anodic processes and larger corrosion products were present. These processes were less intense on the D2 copper electrode, where no anodic activity was observed with CMEA technique, but based on the corrosion products observed we can conclude that both anodic and cathodic processes occurred, indicating net current activity.

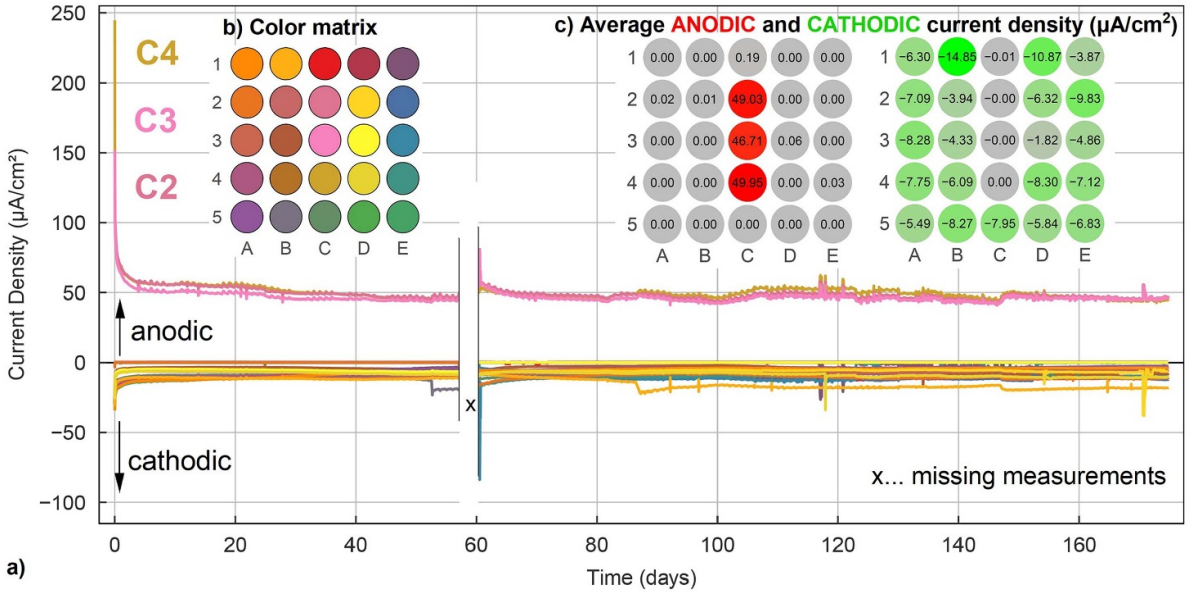

Figure 6. (a) Evolution of the current densities in the CMEA-CS-3 sensor with a Cu/CS ratio of 22/3 over 176 d of exposure to the bentonite mixture in an oxic environment, (b) color matrix of a 5 × 5 grid, and (c) average anodic and cathodic current densities of individual electrodes over 176 d.

Continuous corrosion monitoring of the CMEA-CS-3 sensor with a Cu to CS ratio of 22/3 under a bentonite mixture in an oxic environment.—The CMEA-CS-3 sensor with a Cu/CS ratio of 22/3 designed for the long-term monitoring of galvanic corrosion between copper and carbon steel is shown in Fig. 6. The CMEA-CS-3 sensor was monitored for 176 d under a bentonite mixture in oxic conditions.

In the CMEA-CS-3 sensor with three steel electrodes (C2, C3, and C4) an initial peak occurred in the CS electrodes after bentonite was poured over them, as shown in Fig. 6a. The highest anodic peak, observed in the C4 electrode, exceeded 240 μA cm^{-2}. The peaks in the C2 and C3 electrodes reached 122 μA cm^{-2} and 152 μA cm^{-2}, respectively. The current in all three of the carbon steel electrodes decreased rapidly, and within four days the anodic activity dropped to around 50 μA cm^{-2}, where it then remained stable. After 58 d of exposure, the experiment was interrupted due to the institute's corrections to the electrical network. The electrodes were decoupled for 3 d, during which a different corrosion behavior was temporarily established, with each electrode acting independently. When the electrodes were reconnected, the corrosion behavior returned relatively quickly to the coupled state and continued as before. As shown in Fig. 6, after the electrodes were coupled, a spike in current density occurred (above 100 μA cm^{-2} for the CS electrodes), but within one day the current density decreased to approximately 50 μA cm^{-2}, as it was before the interruption. Considering the total exposure time, the three-day interruption did not represent a significant disturbance to the measurement. Cracking of the bentonite was observed after exposure due to drying; however, this did not significantly affect the measured current density of the CS electrodes. The anodic current density remained stable throughout the measurement, likely because the larger anodic surface area compared to the smaller cathodic surface area limits the driving force of cathodic reactions, making the system less sensitive to changes such as crack formation.

Figure 6c presents the average anodic and cathodic current densities. The average anodic current density for the C2 CS electrode is 49 μA cm^2, which correlates with the estimated corrosion rate of 0.56 mm year^{-1} calculated using Eq. 1. The corrosion rates for the C3 and C4 CS electrodes were 0.54 mm year^{-1} and 0.63 mm year^{-1}, respectively. The damage to the CS electrodes was estimated from the CMEA data using Equation 2. The corrosion damage for electrodes C2, C3, and C4 was 271 μm, 258 μm, and 276 μm, respectively.

To verify the corrosion rate and determine the damage to the electrodes in the CMEA-CS-3 sensor, μ-CT analysis was performed. For the CMEA-CS-1 sensor, the corrosion damage measured by μ-CT was 10% higher than that obtained by the CMEA technique. Therefore, it is reasonable to assume that the corrosion damage estimated by μ-CT will also be higher in the CMEA-CS-3 sensor, and, as such, that the corrosion rate obtained with the CMEA technique would be an underestimation.

The total damage volumes of the C2, C3, and C4 CS electrodes were $62.5{\cdot}10^6$ μm^3, $62.4{\cdot}10^6$ μm^3, and $63{\cdot}10^6$ μm^3, respectively. These values correspond to corrosion damages of 318 μm for C2, 318 μm for C3, and 321 μm for C4. Table I presents a comparison of the corrosion damage measured by each technique (CMEA and μ-CT). The data suggests that the corrosion rates are slightly underestimated, as the levels of damage observed by μ-CT are approximately 10% to 22% higher than those measured using the CMEA technique.

In galvanic corrosion, the intensity of the corrosion processes is influenced by several parameters, with the main parameter being the ratio between the surface areas of the anode and the cathode. If the surface area of the cathode is larger than that of the anode, the intensity of the corrosion processes increases, as the galvanic couple is under cathodic control. A larger cathodic area allows more reduction processes, which accelerates the corrosion of the anode.[5,6,40,41] The influence of the area ratio of steel galvanically coupled to copper has been investigated in different chloride solutions. As the ratio increased from 1:1 to ≈ 2500:1 the corrosion rate of CS increased indicating that the galvanic corrosion rate is under cathodic control.[5] The influence of the bentonite layer on galvanic corrosion between copper and steel has also been investigated.[6] In the presence of bentonite, the rate-controlling reaction was still the reduction of O_2, but the bentonite hinders its diffusion and shifts to a more negative E_g, and a drop in i_g was observed.[6]

The intensity of the galvanic corrosion in the CMEA-CS-3 sensor (with three CS electrodes) was lower than that in the CMEA-CS-1 sensor (with one CS electrode). In the sensor with one CS electrode, the surface area of the C3 CS electrode was 0.196 mm^2, while the surface area of the cathodic region was 4.70 mm^2. In the sensor with three CS electrodes (C2, C3, and C4), the surface area of the anode was 0.588 mm^2 and the area of the cathode was 4.31 mm^2.

Table I. Comparison of the corrosion damage measured using the CMEA technique and μ-CT for the C2, C3, and C4 CS electrodes in the CMEA-CS-3 sensor.

Technique/Electrode	C2	C3	C4
CMEA	270 μm	258 μm	276 μm
μ-CT	318 μm	318 μm	321 μm

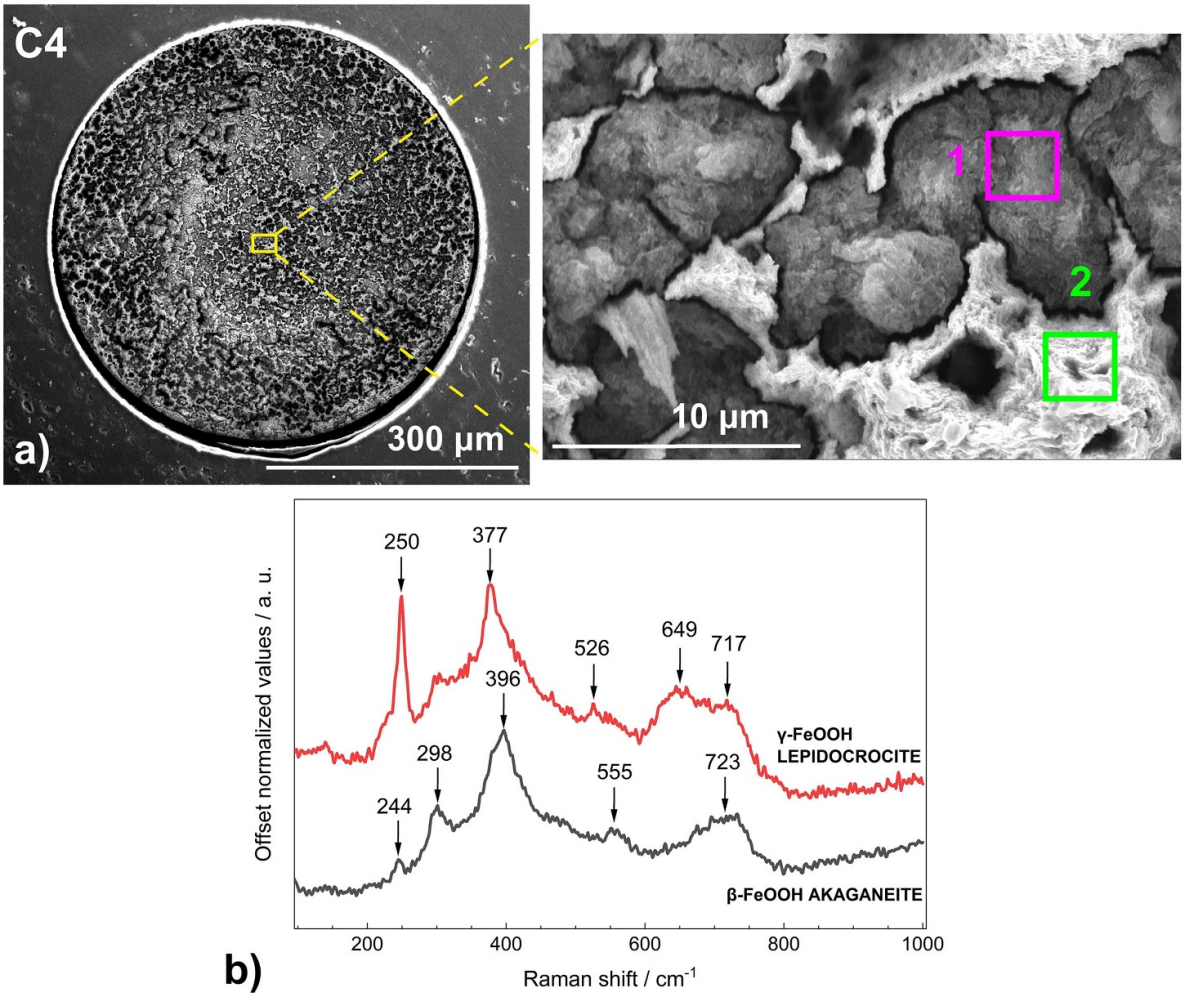

Figure 7. (a) SEM/SE images of the C4 CS electrode at 230 × and 5000 × magnification, and (b) Raman spectra of the C4 CS electrode after exposure to the bentonite mixture in an oxic environment for 176 d.

The anodic activity of the CS electrode in the CMEA-CS-1 sensor, with an anodic surface area of 0.196 mm^2, was 74.7 μA cm^{-2}, while the anodic activity of the CS electrodes in CMEA-3, with a surface area of 0.588 mm^2, was 45.5 μA cm^{-2}. The corrosion rate calculated for the C3 steel electrode in the CMEA-CS-1 sensor was 0.86 mm year^{-1}, compared to 0.56 mm year^{-1} for the CMEA-CS-3 sensor. The results show that the intensity of galvanic corrosion in the system with one CS electrode (C3 in CMEA-CS-1) is 61% higher than in the system with three CS electrodes (C2, C3, and C4 in the CMEA-CS-3 sensor), indicating greater electrochemical activity and a higher degree of material degradation in the case of the CMEA-CS-1 sensor.

The C2, C3, and C4 CS electrodes all had the same morphology, as shown in Supplementary Material Fig. S1. The C4 CS electrode was selected to characterize the corrosion products because it had the highest average anodic activity (49.9 μA cm^{-2}) and the greatest corrosion damage (276 μm). Scanning electron microscopy and Raman spectroscopy were performed, as shown in Fig. 7.

The morphology of the C4 CS electrode is shown in Fig. 7a. Two distinct sites can be identified but EDX analysis revealed similar chemical compositions at the surface. The Fe content was ≈ 97 wt.%, and the O content was ≈2 wt.%. Other elements identified by EDX analysis at sites 1 and 2 were Mn, Cr, Cl, and Cu, all of which were under 1 wt. %. For identification of the corrosion products Raman spectroscopy was performed on the C4 CS electrode following its exposure to a bentonite mixture in an oxic environment. The Raman spectrum, shown in Fig. 7b, confirms that the corrosion products are composed of a mixture of iron oxyhydroxides. The first steel corrosion product identified is lepidocrocite[42] (γ-FeOOH), with bands at 250 cm^{-1}, 377 cm^{-1}, 526 cm^{-1}, and 649 cm^{-1}. The second corrosion product is akaganeite[42] (β-FeOOH), with bands at 298 cm^{-1}, 396 cm^{-1}, 717 cm^{-1}, and 723 cm^{-1}. In contrast

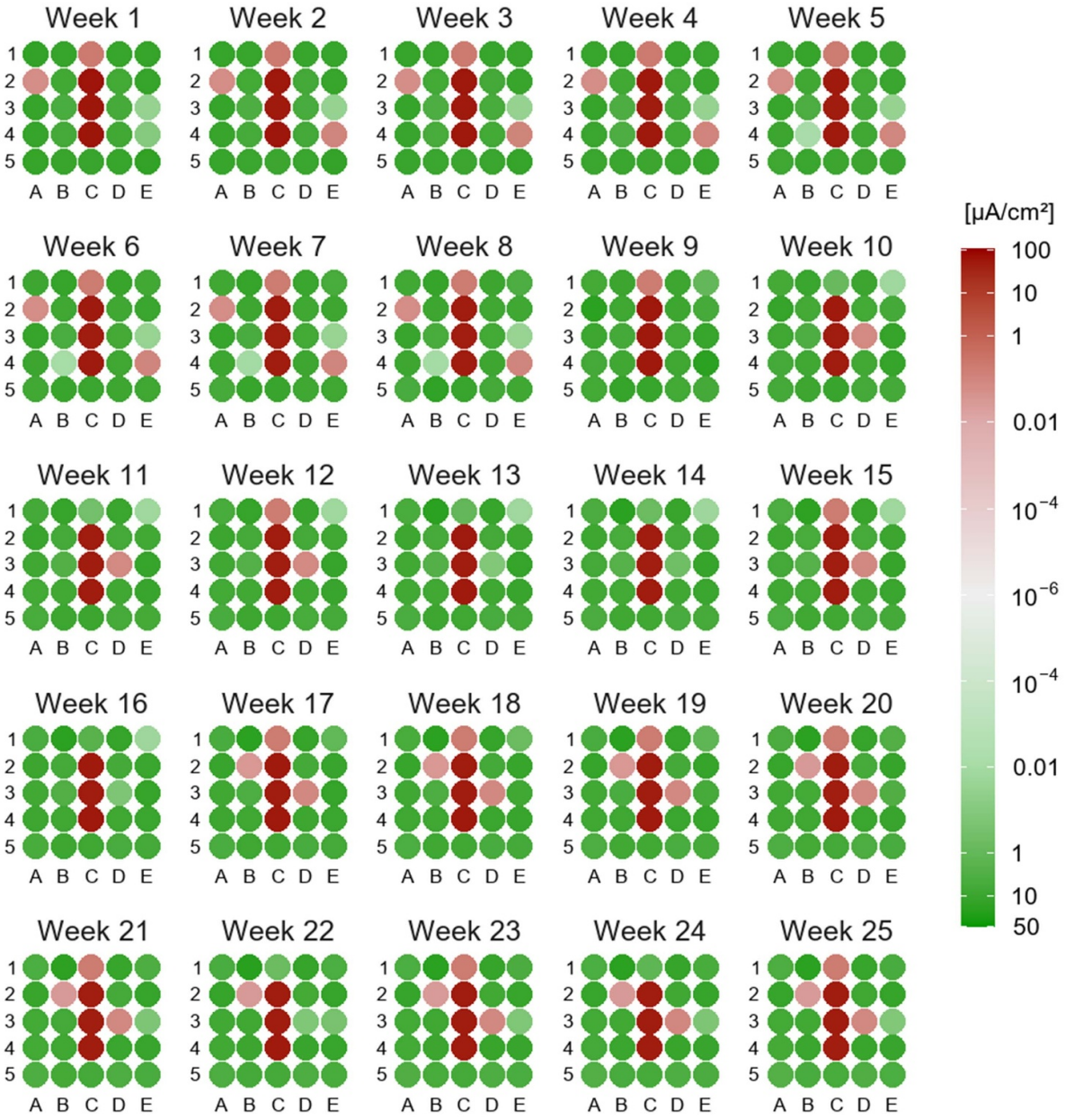

Figure 8. Average anodic (red) and cathodic (green) current densities measured on individual electrodes over each one-week cycle of CMEA-CS-3 sensor over 176 d of exposure to the bentonite in an oxic environment. The color scale is plotted on a logarithmic axis.

to goethite, the presence of lepidocrocite and akaganeite indicates non-protective corrosion products.[4] This can also be related to the evolution of current density. For the sample CMEA-CS-3, the current density of the CS electrodes remains almost constant, at around 50 μA cm^{-2}, from the beginning to the end of the measurements. For the sample CMEA-CS-1, the anodic activity of the C3 CS electrode decreases from the start, and if there were no oxygen ingress, the current density would remain low (below 10 μA cm^{-2}). However, after the current density increased, it began to decrease again, which may indicate the protective nature of goethite.

In the CMEA-CS-1 sensor, the CS electrode acts as the dominant anode, as expected from the behavior of a copper–steel galvanic couple. Among the copper electrodes, only D1 exhibited net anodic activity over the entire exposure of the sensor to the bentonite mixture in an oxic environment, but this activity was almost negligible (Fig. 2c). From Fig. 6c, net activity is visible on some copper electrodes, indicating that both anodic and cathodic processes occur on the surface of the copper electrodes. Fig. 8 shows more detailed average current densities measured in individual electrodes over 25 weeks of exposure of the CMEA-CS-3 sensor to bentonite in an oxic environment (176 d). The main anodes were the CS electrodes, as expected for a Cu–CS galvanic couple. However, more copper electrodes showed net anodic behavior, indicating anodic processes. As seen in Fig. 8, more copper electrodes had net anodic activity compared to the CMEA-CS-1 sensor. During the first few weeks of exposure, copper electrodes A2, C1, and E4 had net anodic activity. They were located at the edge of the array, indicating an edge effect in the multi-electrode array. This observation suggests that, in addition to oxygen reduction sustaining the anodic activity of the CS electrodes, corrosion also occurred on the copper electrodes, indicating the influence of local electrochemical conditions. After interruption of the electrical network, the anodic activity of the

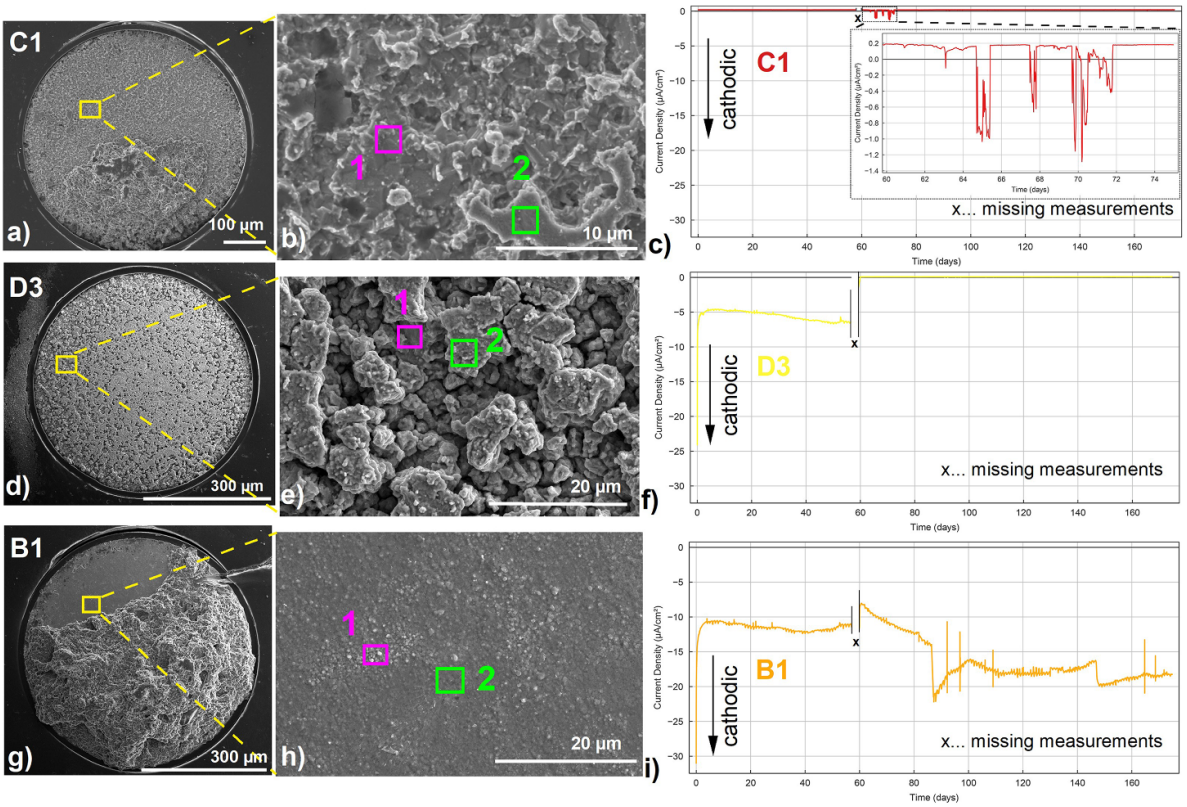

Figure 9. SEM/SE images of the C1 (a), (b), D3 (d), (e), and B1 (g), (h) copper electrodes at 230 × and 5000 × magnification and evolution of the current density for the C1 (c), D3 (f), and B1 (i) copper electrodes after exposure to the bentonite mixture in an oxic environment for 176 d.

Table II. Average anodic and cathodic current densities estimated corrosion rate, and corrosion damage for three different copper electrodes (C1, D3, and B1) in the CMEA-CS-3 sensor over 176 d of exposure to a bentonite mixture in an oxic environment.

CMEA-CS-3 Copper electrode	Average anodic current density (j_{anod} [μA cm^{-2}])	Average cathodic current density (j_{cath} [μA cm^{-2}])	Corrosion rate (v_{corr} [μm year^{-1}])	Corrosion damage (d [μm])
C1	0.19	–0.01	4.4	2.1
D3	0.06	–1.82	1.39	0.67
B1	/	–14.9	/	/

CS electrodes quickly resumed, and copper electrodes also started to behave anodically. These were copper electrodes B2, C1, and D3, which are located near the CS electrodes. Only copper electrode C1 consistently showed net anodic behavior. The presence of three CS electrodes results in a more complex distribution of corrosion behavior, driven by factors such as ohmic potential drop, oxygen consumption, oxygen diffusion, and the local environment. This complexity is evident across the copper electrodes compared to the CMEA-CS-1 sensor, which had only one CS electrode. The anodic activity of the copper electrodes suggests that oxidation processes occurred on their surfaces, which can be confirmed by surface characterization.

In the CMEA-CS-3 sensor, copper electrodes, such as B2, C1, D3, and E4, exhibit anodic activity. These same copper electrodes also showed cathodic activity, suggesting net current activity for the copper electrodes. Three copper electrodes (C1, D3, and B1) are presented in Fig. 9. First, the morphology of the copper electrodes is shown, followed by the evolution of the current density over 176 d of exposure to the bentonite mixture in an oxic environment.

Different copper electrodes with differing behavior are presented in Table II across the entire 176 day period of exposure.

The C1 copper electrode was initially in the anodic region of current density evolution, indicating net anodic processes. After network interruptions and reconnection of the electrodes, the C1 copper electrode showed spikes in the cathodic region, suggesting net cathodic activity and reduction processes. However, after a few days, the net anodic current density was reestablished, and the electrode remained anodic for the rest of the exposure period. The average net anodic current density for the C1 copper electrode was the highest among the copper electrodes, at 0.19 μA cm^{-2}. The corrosion rate calculated from the current density of the C1 electrode was 4.4 μm year^{-1}, and the estimated corrosion damage was approximately 2.1 μm. The D3 copper electrode had the second highest net anodic current density, with an average of 0.06 μA cm^{-2}. Based on the evolution of the current density in Fig. 9f, the D3 copper electrode was initially in the cathodic region. After the network connection was established, the electrode began to act as the anode and remained anodic until the end of the exposure (Fig. 9f). The average net cathodic current density was –1.82 μA cm^{-2}, while the average net anodic activity of the electrode was 0.06 μA cm^{-2}. The most cathodic copper electrode, B1, was adjacent to the most anodic copper electrode, C1. The net cathodic current density of the B1 copper electrode was –14.9 μA cm^{-2}.

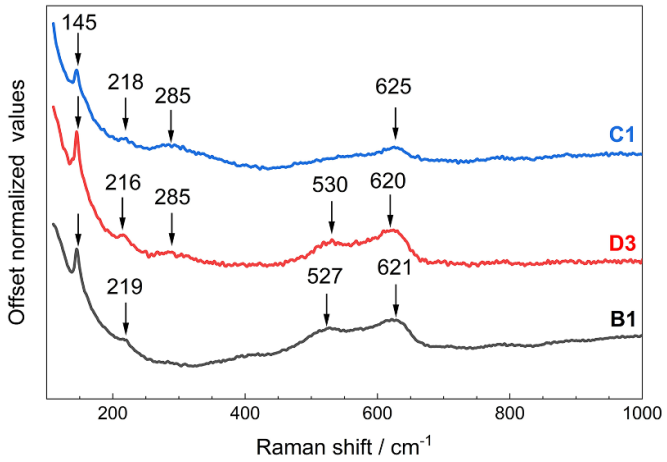

Figure 10. Raman spectra of the C1 (net anodic behavior), D3 (anodic and cathodic behavior), and B1 (net cathodic behavior) copper electrodes after exposure to the bentonite mixture in an oxic environment for 176 d.

Surface characterization of selected copper electrodes was also performed. Fig. 9 shows three of the copper electrodes: B1, C1, and D3.

Different morphologies are observed on the various copper electrodes. The C1 copper electrode exhibited the highest average net anodic current density (0.19 μA cm^{-2}) and damage to the copper electrode is visible in the SEM images (Figs. 9a and 9b). Both large and fine corrosion deposits are present on the surface, but it appears that corrosion products were also removed along with the bentonite. At spot 1, EDX analysis detected 98 wt.% Cu and 2 wt.% O. At spot 2, 95.2 wt.% Cu, 4.2 wt.% O, and a small concentration of S (0.6 wt.%) were detected, indicating corrosion processes involving bisulfide.

Figures 9d and 9e show the D3 copper electrode, which exhibited both anodic and cathodic behavior indicating on net activity. Larger corrosion products are observed on the surface, with smaller deposits on top of the larger ones. EDX analysis at spot 1 showed Cu (93.3 wt.%), O (4.9 wt.%), and S (1.7 wt.%). At spot 2, only Cu (97.7 wt.%) and O (2.3 wt.%) were detected.

For the B1 copper electrode, which was still more than half covered with bentonite, EDX analysis was performed at the upper part of the electrode (Figs. 9g and 9h). Very small deposits are observed on the surface. On these deposits, EDX showed Cu (93.1 wt.%), O (6.1 wt.%), and S (0.27 wt.%), as well as Si (0.12 wt.%) and Ca (0.35 wt.%), indicating the presence of bentonite residue. At spot 2, the Cu content is higher (96.4 wt.%) and the O content lower (3.2 wt.%) than at spot 1. The presence of S is observed at 0.07 wt.%, and Si and Ca are present in low concentrations (0.12 wt.% and 0.22 wt.%).

Raman spectroscopy was performed to characterize the corrosion products on the copper surfaces, as shown in Fig. 10.

All three copper electrodes (C1, D3, and B1) showed the presence of cuprite, with similar peaks at 145 cm^{-1}, 219 cm^{-1}, 530 cm^{-1}, and 621 cm^{-1}. The presence of cuprite is consistent with exposing copper to bentonite in an oxic environment with a high concentration of oxygen. For the C1 and D3 copper electrodes an additional peak was observed. This peak, at around 290 cm^{-1}, indicates the presence of Cu_2S, confirming corrosion processes involving dissolved bisulfide. The detection of Cu_2S shows that sufficient SH^- remained available to react with the copper surface, despite competing reactions with dissolved oxygen and bentonite. Kosec et al.[32] also observed small rounded crystals on the surfaces of copper electrodes, where Raman spectroscopy indicated the presence of cuprite and also identified Cu_2S.

In the CMEA-CS-3 sensor, which contains three carbon steel electrodes (C2, C3, and C4), anodic corrosion processes also occur on the copper electrodes, as confirmed by the presence of corrosion products (Cu_2O, Cu_2S) on the copper electrodes (C1, D3, and B1). Even on the B1 copper electrode, which exhibited net cathodic current density throughout the experiment, Cu_2O was present on the surface, indicating oxidation of the copper. Since corrosion products were observed on the copper electrodes, it can be concluded that both anodic and cathodic processes are occurring on these electrodes. On some copper electrodes, the anodic processes are more intense, as reflected in the evolution of the current density (Fig. 9).

The damage beneath the corrosion products and the bentonite residue were also investigated. The surface morphologies of the copper electrodes examined (C1, D3, and B1) are shown in Fig. 11.

The C1 copper electrode, along with the D3 copper electrode, showed the highest average net anodic activity (0.19 μA cm^{-2} and 0.06 μA cm^{-2}). Raman spectroscopy revealed the presence of Cu_2O and Cu_2S on both electrodes. After removal of the corrosion products and bentonite residue, SEM investigation showed different degrees of roughness (Figs. 11a–11d), while EDX detected only Cu and C on the surfaces of the electrodes. The Cu content was approximately 92 wt.% and the C content around 8 wt.%.

Figure 11f shows the surface of the B1 copper electrode, which had the lowest average current density (–14.85 μA cm^{-2}). Following 176 d of exposure to the bentonite mixture in an oxide environment, the dotted line marks the boundary where bentonite remained adhered to the electrode after removing it with deionized water. More pronounced damage to the adhered bentonite is observed around this boundary. This is also seen on the surface that was covered with bentonite. The damage due to bentonite adhesion is indicated by arrows. Of all the copper electrodes analysed (C1, D3, and B1), however, the B1 copper electrode had the least damaged surface, consistent with the fact that the entire exposure was in the cathodic region of measurement.

Conclusions

Continuous monitoring of galvanic corrosion processes has been successfully demonstrated using the coupled multi-electrode array (CMEA) technique. The study was conducted in the presence of bentonite in an oxic environment. The Cu:CS surface area ratio has been adequately evaluated. The CMEA sensor with one CS elec-

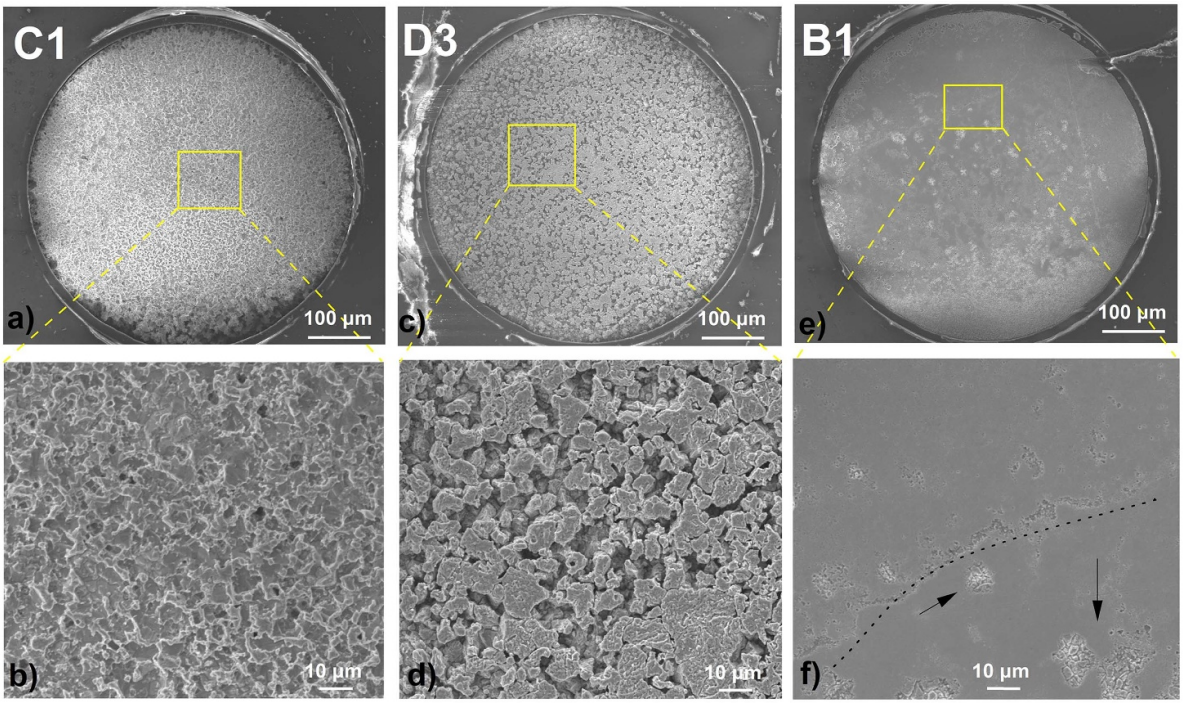

Figure 11. SEM/SE images of the copper electrodes after removing the corrosion products and bentonite residue: the copper C1 electrode (anodic behavior) (a), (b), the copper D3 electrode (anodic and cathodic behavior) (c), (d), and the copper B1 electrode (cathodic behavior) (e), (f).

trode (CMEA-CS-1) was exposed for 186 d, while the CMEA sensor with three CS electrodes (CMEA-CS-3) was exposed for 176 d. The study was conducted in the presence of bentonite in an oxic environment.

(1) Using the CMEA method, the evolution of corrosion processes was successfully monitored, providing spatial and temporal insights into electrochemical behavior.
(2) The effect of the exposed CS surface area relative to the copper surface area was evaluated. A greater corrosion intensity was observed in the sensor with one CS electrode (CMEA-CS-1) compared to the 24 copper electrodes. The corrosion rate of the CS electrode was estimated to be 0.86 mm year^{-1}.
(3) The corrosion rate decreased when a larger CS surface area was exposed relative to the area of the copper surface (i.e., in the CMEA-CS-3 sensor). The exposed surface area of the CS electrodes was 0.588 mm^2. The corrosion rate was estimated to be 0.56 mm year^{-1}, about 38% lower than the corrosion rate for a CS electrode with an area of 0.196 mm^2.
(4) Corrosion damage was estimated using the CMEA technique and μ-CT tomography. μ-CT showed 10%–20% differences in the estimated damage, which can result in an underestimation of the corrosion rate as obtained by the CMEA technique. This difference can be attributed to higher and more intense anodic activity, as would be seen in an environment that is not highly corrosive.
(5) The corrosion products on both samples indicate the presence of oxides. On the CS electrodes, goethite, lepidocrocite, and akaganeite were identified. On the copper electrodes, cuprite was present. On the copper electrodes with net anodic activity, the Raman spectrum also indicated the presence of Cu_2S.
(6) Bentonite strongly adhered to the copper surface on the most cathodic electrode, B1. Bentonite inhibits the transport of corrosive substances, and damage to the copper surface beneath the bentonite may indicate local corrosion processes.

Acknowledgment

The authors acknowledge financial support from the Slovenian Research and Innovation Agency—ARIS through research program No. P2-0273 and Young Researcher financing No. 56914.

Data availability statement

The research data is available at: http://hdl.handle.net/20.500.12556/DiRROS-30541.

ORCID

Klara Kregar https://orcid.org/0009-0004-5370-6653
Miha Hren https://orcid.org/0000-0001-5826-0508
Aleš Nagode https://orcid.org/0000-0003-2175-0516
Tadeja Kosec https://orcid.org/0000-0001-6790-1880

References

1. Z. Ahmad, *Principles of Corrosion Engineering and Corrosion Control*, p. 120, Butterworth-Heinemann, Oxford, UK (2006).
2. B. O. Hasan, *J. Pet. Sci. Eng.*, **124**, 137 (2014).
3. R. W. Revie, *Uhlig's Corrosion Handbook*, 3rd ed, Canmet, Ottawa, Ontario (2011).
4. B. O. Okonkwo, H. Ming, F. Meng, J. Wang, X. Xu and E.-H. Han, *J. Nucl. Mater.*, **548**, 152853 (2021).
5. T. E. Standish, L. J. Braithwaite, D. W. Shoesmith and J. J. Noël, *J. Electrochem. Soc.*, **166**, C3448–C55 (2019).
6. L. Braithwaite, K. Albrechtas, D. Zagidulin, M. Behazin, D. Shoesmith and J. J. Noël, *J. Electrochem. Soc.*, **169**, 051502 (2022).
7. Z. Su, J. Pang, Y. Xin, N. Liu, X. Liu, X. Han, W. Xu and X. Chen, *J. Electrochem. Soc.*, **173**, 091504 (2026).
8. X. Li, X. Pan, F. P. Filice, D. Zagidulin, J. Chen, M. Behazin, S. Matin and J. J. Noël, *Electrochim. Acta.*, **532**, 146505 (2025).
9. ISO/DIS 23449, *Corrosion of Metals and Alloys—Multielectrode Arrays for Corrosion Measurement* (2020).
10. L. Yang, N. Sridhar, O. Pensado and D. S. Dunn, *Corrosion*, **58**, 1004 (2002).
11. F. Bocher, F. Presuel-moreno and J. R. Scully, *J. Electrochem. Soc.*, **155**, C256 (2008).